Macromolecules

pubs.acs.org/Macromolecules
Article

Cytocompatible Triblock Copolymers with Controlled Microstructure Enabling Orthogonally Functionalized Bio-polymer Conjugates

Kerstin Halama, Molly Tzu-Yu Lin, Andreas Schaffer, Marvin Foith, Friederike Adams, and Bernhard Rieger*

Cite This: *Macromolecules* 2024, 57, 1438–1447
Read Online

ABSTRACT: α,ω-Functionalized block copolymers create various opportunities across myriads of applications such as linkers for targeted drug delivery systems. Combining them with the exceptional properties of polyvinyl phosphonates, such as high control over polymer architecture and biocompatibility, further reinforces their benefits. This study focuses on synthesizing the α-allyl-ω-TMSpropargyl-*block-co*-polymer P(DAlVP-DEVP-DPrTMSVP) by rare-earth metal-mediated group transfer polymerization. The monomers involved in this process are functionalized diallyl vinyl phosphonate (DAlVP) and dipropargyl vinyl phosphonate (DPrTMSVP), as well as hydrophilic diethyl vinyl phosphonate (DEVP), enabling the incorporation of diverse functionalities into the polymer structure. Click chemistry, including azide-alkyne cycloaddition (AAC) and thiol-ene reactions, facilitates specific and controlled modifications of polymer side chains. Various model substrates, such as benzyl azide, 3-azido-7-hydroxycoumarin, and cysteamine, show the scope of these modifications. The potential in (bio)medical applications is proven with the polymer−biomolecule conjugate α-cholesteryl-ω-folate-*block-co*-polyvinyl phosphonate, exhibiting remarkable biocompatibility. Our versatile approach also establishes a synthetic platform for drug delivery systems, for instance, in targeted therapy.

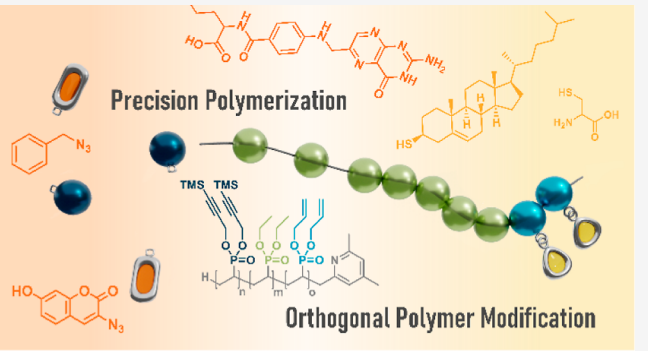

1. INTRODUCTION

Precisely defined and highly functionalized polymers exhibit a high potential in various applications, including biomedical administrations and delivery systems.[1−3] In addition to forming amphiphilic block copolymer-based systems such as micelles and polymersomes, there is great interest in the surface modification of liposomes and polymersomes using specially designed polymer substrate conjugates.[3−7]

One extensively utilized polymer for these purposes is poly(ethylene glycol) (PEG), which is well established as a precursor for therapeutic agents and highly valuable in designing targeted drug delivery systems. PEGylation, the covalent and noncovalent attachment of PEG to different biologically relevant motifs, offers several advantages, such as increasing half-life, reducing immunology, improving solubility, and enhancing stability.[8] PEG also plays a crucial role in site-specific targeting therapeutics and enables the modification of nanoparticles.[9,10] Functionalized macromolecule conjugates are often based on precursor polymers with (different) functional end groups, including both homo (same functional groups on both chain ends) and hetero bifunctional (different functional moieties) systems achieved through initiator/terminating agents or by postpolymerization approaches.[11,12]

Another option for equipping linear polymers with multifunctional units is using triblock copolymers of the ABC type, allowing the incorporation of three different blocks with distinct functionalities and properties.[13] This structure provides a broad range of synthetic options for the sequential, orthogonal functionalization of the blocks with varying functional groups and the potential to access self-assembled nanostructures.[14,15] Achieving precise control over the distribution and placement of functional moieties along the macromolecular backbone offers the opportunity for well-defined polymer conjugates through targeted orthogonal modification.

"Click" chemistry, introduced by Sharpless and co-workers in 2001, shows a valuable concept for subsequent functionalization of various polymeric materials.[15,16] It provides high

Received: November 2, 2023
Revised: January 18, 2024
Accepted: January 24, 2024
Published: February 6, 2024

https://doi.org/10.1021/acs.macromol.3c02238
Macromolecules 2024, 57, 1438−1447

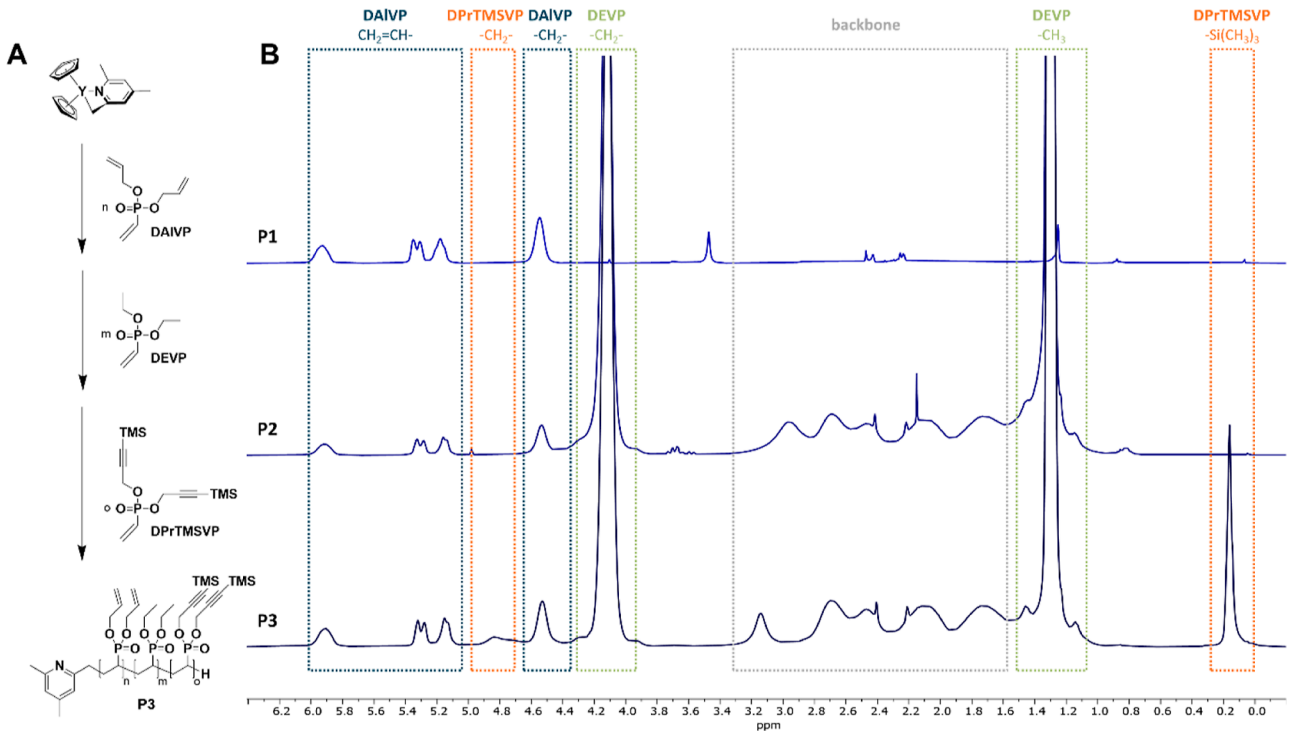

Figure 1. Sequential REM-GTP of DAlVP, DEVP, and DPrTMSVP with the CH-bond activated species of $Cp_2YCH_2TMS(thf)$ at room temperature (A). Comparison of ^1H NMR spectra (B) for P(DAlVP) **P1**, P(DAlVP-DEVP) **P2**, and P(DAlVP-DEVP-DPrTMSVP) **P3**. ^1H NMR signals of monomers DAlVP (blue), DEVP (green), and DPrTMSVP (orange) are highlighted.

regio- and stereoselectivity, excellent yields under mild reaction conditions, and the possibility to obtain the final structure in few simple steps in a high-yield and reasonable time scale.[15,17] "Double click reactions" enable the orthogonal functionalization of macromolecules by utilizing two chemically and mechanistically different click reactions to ensure the targeted modification of the polymer side chains.[17−19] One promising strategy is the combination of a thiol-ene click reaction and azide-alkyne cycloaddition (AAC).

Polyvinyl phosphonates also provide a versatile platform for functionalized polymers and enhance properties in new and smart materials. These macromolecules possess notable characteristics, including high biocompatibility,[20−24] good solubility in water, and a tunable lower critical solution temperature (LCST).[25] Moreover, the presence of two functionalizable motifs per monomer unit allows doubling of the attached molecules per repeating unit, resulting in a higher loading capacity. Our group has successfully achieved well-defined, high molecular-weight polyvinyl phosphonates via living rare-earth metal-mediated group transfer polymerization (REM-GTP).[25−30] This method enables excellent control over the polymer microstructure in terms of copolymer composition and the creation of block structures with various functional monomers while maintaining a narrow polydispersity. Besides, various modification options are available, including end-group functionalization with different initiators functionalized with azides, allyl groups, or other protected reactive groups.[21,31−34] Moreover, modifying polymers through postpolymerization functionalization or incorporating diverse functional monomer units is feasible.[35,36] Furthermore, amphiphilic block copolymers containing polyvinyl phosphonates have been studied for their micellar formation, loading and release behavior, and modification options.[20,23,37−39] Postpolymerization functionalization also allows the attachment of different biologically active substrates to the polymer. The successful synthesis of a polymer−biomolecule conjugate involving folic acid or cholesterol has been achieved via thiol-ene click chemistry on a vinyl-containing polymer end group, followed by investigations on the localization of these polyvinyl phosphonate conjugates in HMEC-1 cells.[21,40]

This study capitalizes on the advantages of precision polymerization via REM-GTP for the selective introduction of allyl and propargyl moieties into terpolymers, which serve as flexible anchors for the selective incorporation of (biological) substrates.[41] To this end, monomers containing functional groups, such as diallyl vinyl phosphonate (DAlVP, **1**) and di trimethylsilyl propargyl vinyl phosphonate (DPrTMSVP, **3**), are chosen. By combining these monomers with diethyl vinyl phosphonate (DEVP, **2**), which contributes to the enhanced water solubility of the final polymer structure, the *block-co*-polyvinyl phosphonate P(DAlVP-DEVP-DPrTMSVP) **P3** is synthesized.

These α,ω-block copolymers enable orthogonal functionalization through AAC followed by a thiol-ene click reaction, opening the pathway for site-specific introduction of different model substrates. The postpolymerization functionalization and sequential modification of the propargyl groups containing polyvinyl phosphonate **P4** is tested using aromatic benzyl azide and the dye 3-azido-7-hydroxycoumarin as model substrates. Furthermore, the functionalization of the allyl groups with cysteamine is confirmed. To advance toward a biological application of these polymers, modification with cholesterol, an essential compound of the cell membrane,[42,43] and folic acid, which specifically targets the folic-acid receptor (FR-α) and is a well-known drug-delivery targeting group, are investigated.[44−46]

https://doi.org/10.1021/acs.macromol.3c02238
Macromolecules 2024, 57, 1438−1447

2. RESULTS AND DISCUSSION

2.1. Synthesis of α-Allyl-ω-TMSpropargyl-*block-co*-polyvinyl Phosphonate P(DAlVP-DEVP-DPrTMSVP). The controlled incorporation of allyl and propargyl functionalized monomers to form the hetero terpolymer is facilitated by the living character of REM-GTP, allowing a sequential addition of different monomers due to the constant coordination of the growing polymer chain at the catalyst center. After quantitative C−H bond activation of $Cp_2YCH_2TMS(thf)$ with 2,4,6-trimethylpyridine in toluene is confirmed via nuclear magnetic resonance (NMR) spectroscopy, the initial monomer DAlVP is introduced.[47] A limited number of five monomer units is employed to maintain the water solubility of the final polymer. Consequently, the hydrophilic DEVP core is polymerized before introducing the newly developed vinyl phosphonate DPrTMSVP (Figure 1A). To avoid catalyst decomposition by the acidic proton of the propargyl group upon polymerization, the monomer is previously protected with a trimethylsilyl (TMS) group. This enables the polymerization of a third short polymer block, consisting of propargyl-functionalized vinyl phosphonate **3**, thereby introducing a second modification handle and, finally, the synthesis of α-allyl-ω-TMSpropargyl-*block-co*-polymer **P3**.

To verify the block structure of polymer **P3**, the conversion of each monomer is assessed via NMR after every polymerization step (Figure 1B). The disappearance of the vinyl group in the ^{1}H NMR spectra and the absence of the monomer signal in the ^{31}P NMR spectra indicate complete monomer conversion (Figure S5). This allows for the addition of the following monomer. While the first monomers, DAlVP and DEVP, exhibit living character and achieve full conversion, the polymerization of DPrTMSVP does not proceed to full conversion. It is assumed that although the polymerization is the preferred reaction, the trimethylsilyl-1-properyl side chain of DPrTMSVP can also interact with the catalyst through C−H activation at the CH_2-position, thereby terminating the polymerization process.[48] Nonetheless, incorporating an adequate amount of propargylic-modified monomer **3** into the terpolymer **P3** is possible. The ^{1}H NMR spectra display signals indicative of the allylic side groups in the range of 5.04 to 5.87 ppm (DAlVP), as well as the trimethylsilyl protecting group at 0.13 ppm (DPrTMSVP). Furthermore, the CH_2 group of the respective monomers in **P3** can be observed at 4.08 (DEVP), 4.49 (DAlVP), and 4.79 ppm (DPrTMSVP), enabling the precise determination of the exact monomer composition.

By correlating the above signals with those from the trimethylpyridine initiator, it becomes feasible to determine the monomer composition of DAlVP/DEVP/DPrTMSVP = 5:110:2 through spectral analysis. Additionally, successful polymerization toward **P3** and the absence of homopolymers are confirmed using diffusion-ordered NMR spectroscopy (DOSY-NMR) (Figure S6). Furthermore, the determination of the number-average molecular weight (M_n) and narrow polydispersity (PDI) for the polymers **P2** and **P3** is carried out via size-exclusion chromatography multiangle light scattering (SEC-MALS) (Figures S7 and S8). Dynamic light scattering (DLS) determines that terpolymer **P3** undergoes self-aggregation into micelles due to the hydrophobic nature of the trimethylsilyl group (Figure S9). Comparing DLS measurements between polymers **P2** and **P3** reveals that the diblock copolymer **P2** does not exhibit self-assembly behavior, whereas **P3** forms micelles with an approximate size of 100 nm (Figure 2B).

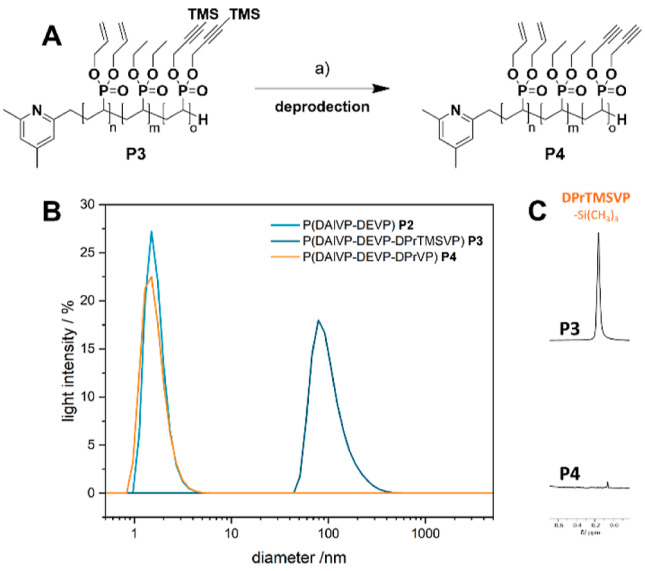

Figure 2. Overview of deprotection of DPrTMSVP in terpolymer **P3**. Conditions (A): (a) K_2CO_3, rt, and overnight [MeOH]. DLS measurements (B) of the polymers **P2** (light blue), **P3** (dark blue), and **P4** (orange) and the extract of the ^{1}H NMR spectra (C) of **P3** and **P4**.

2.2. Deprotection. Before functionalization, the removal of the trimethylsilyl group from the PDPrTMSVP block is required to give access to the desired polymer−substrate conjugates. For the deprotection of the propargyl groups, **P3** is dissolved in methanol, followed by the addition of potassium carbonate. The reaction mixture is stirred at room temperature overnight. The reaction demonstrates full conversion, as confirmed by ^{1}H NMR analysis, where the signals of the TMS group at 0.13 ppm and the CH_2 group at 4.79 ppm disappear entirely (Figures 2C and S10). The SEC-MALS analysis of polymer **P4** provides evidence that the polymer backbone remains unaffected by the reaction conditions and is fully preserved (Figure S13). The DLS measurements confirm no micelle formation in polyvinyl phosphonate **P4** (Figure 2B). To sum up, the results indicate the successful and complete deprotection of the propargyl groups.

2.3. Orthogonal Functionalization of α-Allyl-ω-propargyl-*block-co*-polyvinyl Phosphonate. After successfully synthesizing polyvinyl phosphonate **P4** as an unmodified polymer with well-defined quantities of functionalized monomers, the subsequent step involves testing the orthogonal functionalization of **P4**. To ensure the targeted introduction of diverse substrates, modifying the propargyl groups through AAC is beneficial before performing thiol-ene click reactions on the allyl groups (Figure 3). This approach prevents unwanted thiolyne click reactions between the propargyl groups and the utilized thiols. To screen the AAC, benzyl azide (**4**) is employed as a model substrate due to its distinct aromatic signals in ^{1}H NMR spectroscopy.

The modification of the alkyne groups of the polymer **P4** through AAC is achieved via thermal activation following the Huisgen method.[49] The thermal activation approach successfully eliminates the need to deal with potential metal catalyst contaminations, which would be particularly crucial for later

https://doi.org/10.1021/acs.macromol.3c02238
Macromolecules 2024, 57, 1438−1447

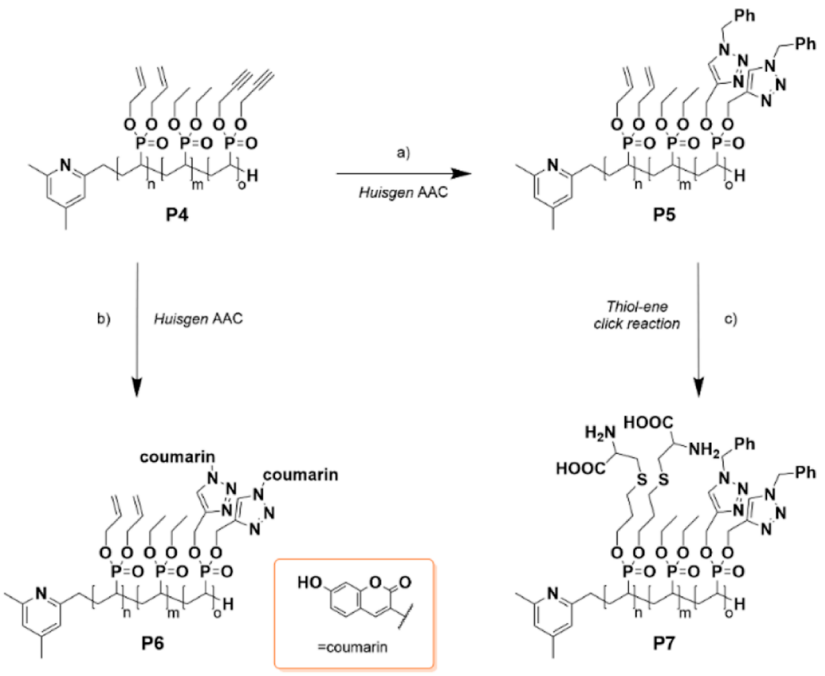

Figure 3. Overview of the synthetic pathway of postpolymerization functionalization of polyvinyl phosphonate **P4**. (a) Benzyl azide (**4**), 110 °C, overnight [DMF], (b) 3-azido-7-hydroxycoumarin (**5**), 110 °C, overnight [DMF], and (c) cysteine (**6**), ACPA, 70 °C, overnight [THF/MeOH].

biomedical applications. Consequently, the polymer and azide derivative **4** are heated overnight to facilitate the reaction. Upon purification, the ^{1}H NMR spectrum reveals a signal ranging from 7.24 to 7.69 ppm, indicating the presence of aromatic protons from the conjugated benzylic group. Furthermore, the effectiveness of the postpolymerization functionalization can be assessed by the weak signal at 8.57 ppm, corresponding to the newly formed triazole (Figure S19). However, due to the low proportion of substrate molecules attached to the polymer and their weak signals, a quantitative analysis of the reaction is not feasible. Nevertheless, the confirmation of successful side-chain functionalization can be inferred based on additional evidence from DOSY-NMR experiments (Figure 4A). It can also be shown that modifying the polymer by the method above did not lead to decomposition of the parent block copolymer (Figures S20–S22). Additionally, the cycloaddition of propargyl groups in polyvinyl phosphonate is confirmed by coupling a water-soluble azide-containing dye, specifically 3-azido-7-hydroxy-coumarin (**5**). This verification is conducted under reaction conditions identical to those of the previous Huisgen click reaction with benzyl azide **4**, and the resulting product is purified via dialysis against water. The successful synthesis of polyvinyl phosphonate **P6** is demonstrated using ^{1}H NMR spectroscopy, wherein the spectrum exhibited aromatic signals ranging from 6.62 to 7.79 ppm, as well as the newly formed triazole signal around 8.47 ppm (Figure S23). Additionally, the DOSY-NMR spectrum confirms the successful conjugation by presenting identical diffusion coefficients for the signals corresponding to the polymer and substrate **5** (Figure 4B). Furthermore, the dye-functionalized polymer **P6** is subjected to absorption (Figure 4C) and fluorescence (Figure 4D) spectroscopy. The absorption spectrum unveils an absorption band at approximately 250 nm and another band at 320 nm, which indicates the conjugate dye **5**. The emission spectrum exhibits a prominent fluorescence band at 490 nm. Collectively, these spectra provide further evidence supporting the presence of the dye within the polymer. To conclude, the functionalization of the propargyl group via Huisgen cycloaddition is achieved on the block copolymer backbone.

Following the introduction of substrates through azide-alkyne cycloaddition, the allyl groups undergo targeted modification by a second structural motif via the thiol-ene click reaction. For this purpose, the amino acid L-cysteine (**6**) is chosen as a thiol, which can also be used for coupling different modified amino acid sequences and thus opens the possibility of peptide functionalization of polyvinyl phosphonates.[50,51] For the modification, the radical reaction of polyvinyl phosphonate **P5** and substrate **6** is initiated by the water-soluble initiator 4,4′-azobis(4-cyanopentanoic acid) (ACPA). In contrast to previous studies,[35] only 1.2 equiv of cysteine is used for each allyl group present in the polymer to prevent thiol-yne click side reactions with unreacted propargyl groups. The success of the synthesis is determined by the NMR analysis of the purified polymer after dialysis. In the ^{1}H NMR spectrum, the signals assigned to the allyl groups at 4.60, 5.46–5.20, and 6.01 ppm have disappeared completely, suggesting quantitative conversion of the allyl groups (Figure S10).

2.4. Application-Oriented Approach—*α*-Cholesteryl-*ω*-folate-*block*-*co*-polyvinyl Phosphonate. Drawing inspiration from the successful end-group postpolymerization functionalization of PDEVP with folic acid (FA) and cholesterol and considering the diverse applications of PEG-modified biomolecules, we synthesize an *α*-cholesteryl-*ω*-folate-*block*-*co*-polyvinyl phosphonate (Figure 5).[21,52,53] This novel copolymer confirms the sequential functionalization strategy based on orthogonal click reactions for the creation of biologically active systems. In this context, coupling of folic acid to the polymer through the radical thiol-ene click reaction is not possible due to the role of FA as a free radical scavenger.[54] Alternatively, attachment of the folic acid

https://doi.org/10.1021/acs.macromol.3c02238
Macromolecules 2024, 57, 1438−1447

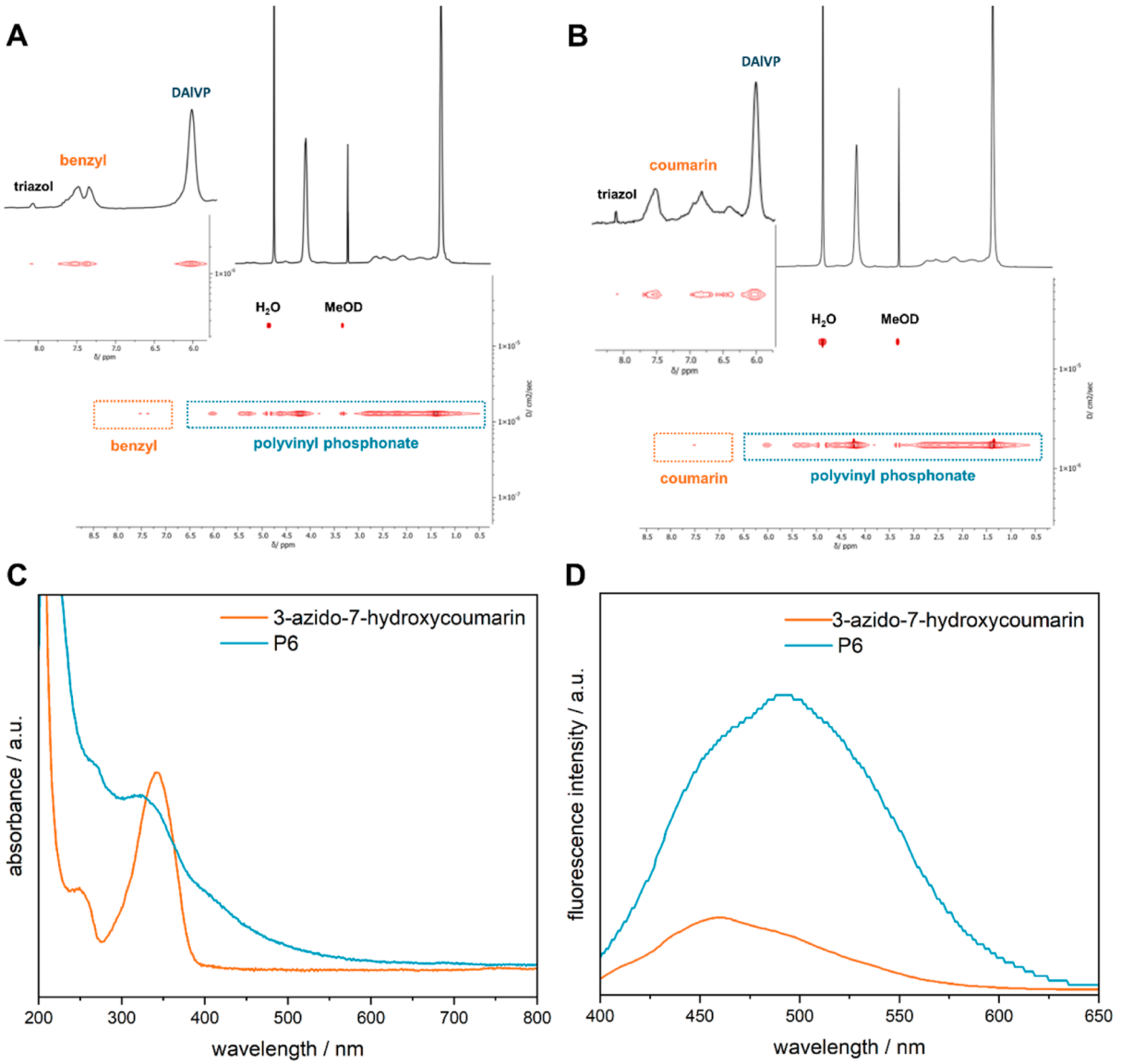

Figure 4. DOSY-NMR spectra of polyvinyl phosphonate **P5** (A) and **P6** (B). Polyvinyl phosphonate (blue) and substrates (orange) are highlighted. UV−vis (C) and fluorescence (D) spectra of **P6** (blue) and 3-azido-7-hydroxycoumarin (orange).

derivative to the polymer does not exhibit a modification of the allyl groups with a second substrate in subsequent thiol-ene click reactions due to the above-mentioned reasons.

Therefore, we initiated the functionalization process by modifying the protected terpolymer **P3** through a thiol-ene click reaction with thiocholesterol (Chol-SH, **7**). To prevent thiol-ene click reactions with the propargyl groups present in the polymer, we apply the protected terpolymer **P3**, in which TMS groups still shield the mentioned functional groups.[55−57] Deprotection of these moieties is performed after functionalization of the allyl bonds. Additionally, we use only 0.9 equiv of cholesterol **7** relative to the allylic groups in the polyvinyl phosphonate during the thiol-ene click reaction. This approach avoids excessive thiols that can react with the alkyne groups. Moreover, a high degree of functionalization negatively affects the solubility of the polymer−biomolecule conjugate and hinders further applications. In the experiment, terpolymer **P3** reacts with thiocholesterol in the presence of the photoinitiator 2,2-dimethoxy-2-phenylacetophenone (DMPA). ^{1}H NMR spectroscopy of polyvinyl phosphonate **P8** demonstrates 75% conversion of the allylic side groups by comparing the spectrum with polymer **P3**. This conversion is confirmed by the decrease in signals corresponding to the allyl groups in the range of 5.04 to 5.87 ppm and the prominent signals of the cholesterol methyl groups from 0.81 to 0.99 ppm (Figure 6).

Additionally, DOSY-NMR investigations of polyvinyl phosphonate **P8** demonstrate that the cholesterol moiety, as well as the polymer signals, exhibits the same diffusion coefficient (Figure S38). The cholesterol-functionalized polyvinyl phosphonate **P8** is not soluble in water due to the presence of two hydrophobic functionalized polymer chain ends, namely, the TMS groups on one side and the lipophilic cholesterol conjugates on the other.

Before the modification with folic acid, the propargyl groups of the polymer **P8** are subjected to deprotection of the TMS groups, following the same procedure as that for polyvinyl phosphonate **P3**. The complete conversion is confirmed for polymer **P9** via ^{1}H NMR spectroscopy (Figure 6). Additionally, the DLS analysis demonstrated that upon the removal of the hydrophobic TMS groups, the polyvinyl phosphonate

https://doi.org/10.1021/acs.macromol.3c02238
Macromolecules 2024, 57, 1438−1447

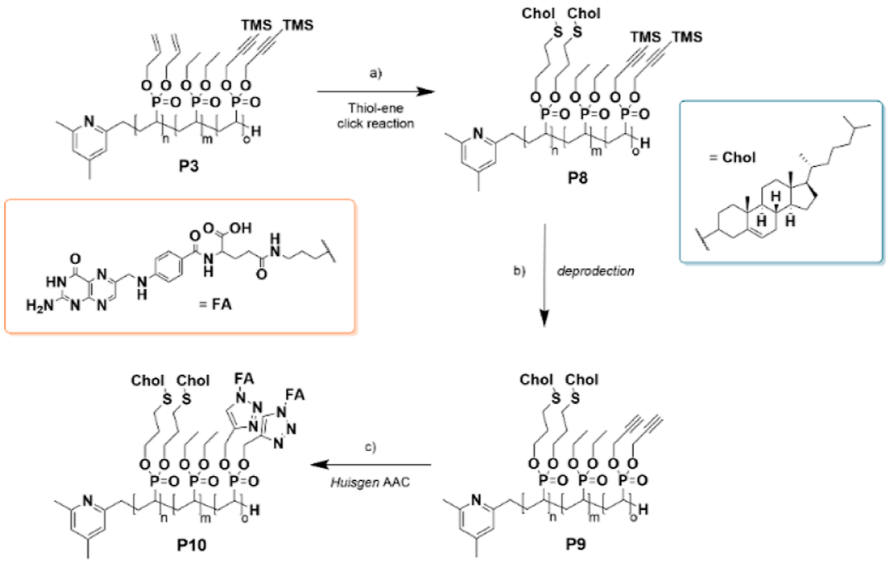

Figure 5. Overview of the synthetic pathway of orthogonal functionalization of terpolymer **P3**. (a) Thiocholesterol (7), DMPA, rt, λ = 365 nm, overnight [THF/MeOH], (b) K_2CO_3, rt, overnight [MeOH], and (c) folic acid azide (**8**), 110 °C, overnight [DMF].

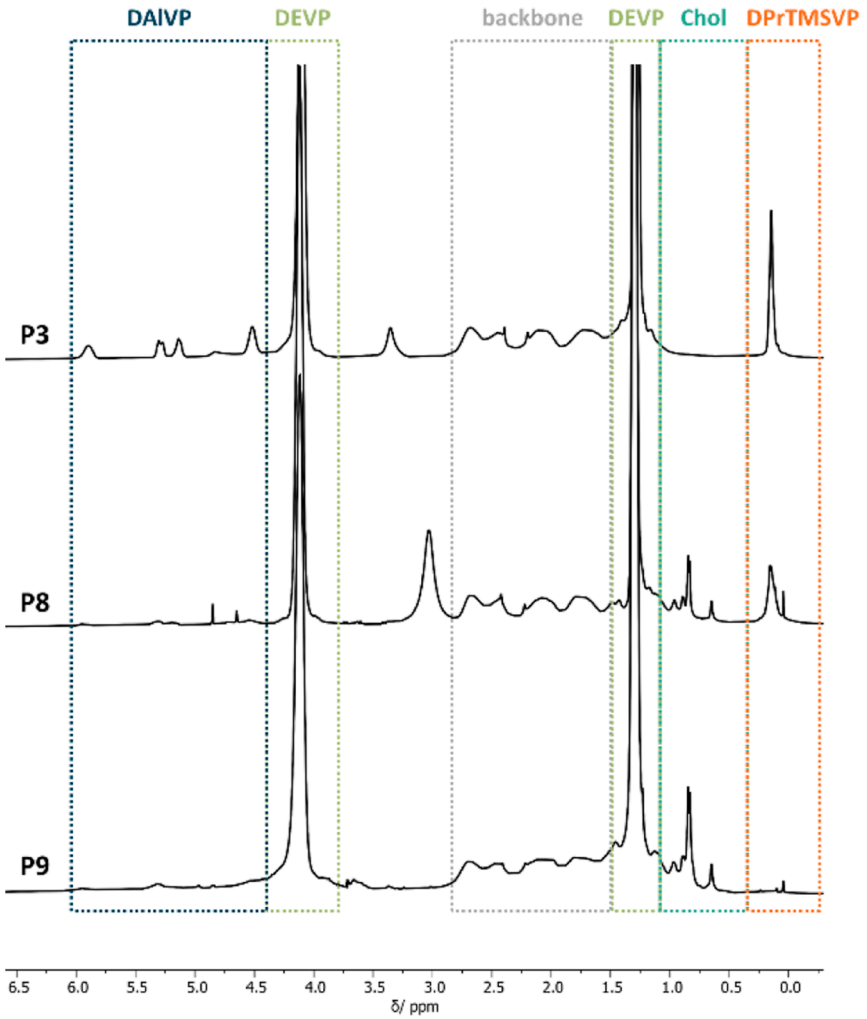

Figure 6. Comparison of ^{1}H NMR spectra of the polymers **P3**, **P8**, and **P9**. Monomers DAlVP (blue), DEVP (light green), DPrTMSVP (orange), as well as cholesterol (dark green), are highlighted.

regained its amphiphilic nature, forming micelles. Notably, the core of the micelles is constituted by the cholesterol-modified block of the polymer (Figure S18). Following the deprotection of the propargyl groups, azido folate **8** needs to be attached to

https://doi.org/10.1021/acs.macromol.3c02238
Macromolecules 2024, 57, 1438−1447

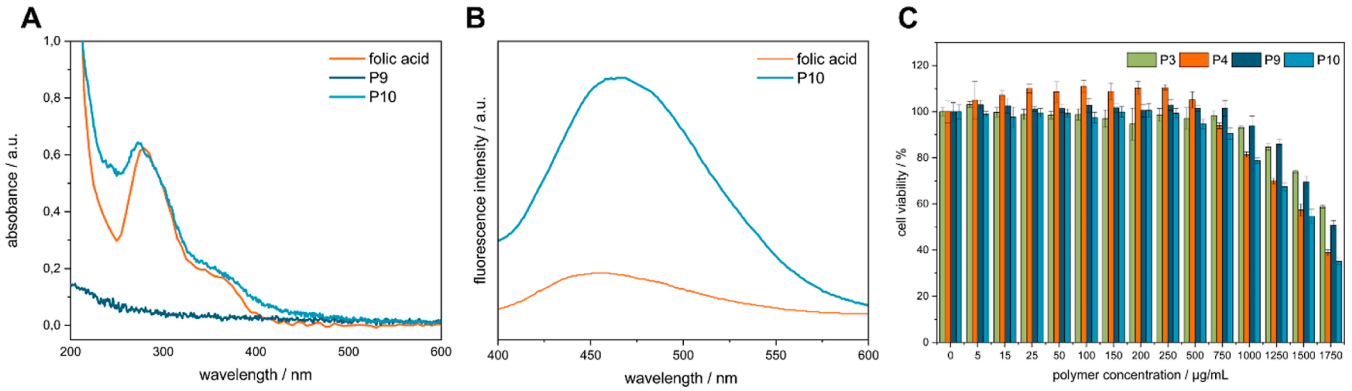

Figure 7. UV−vis (A) and fluorescence (B) spectra of polyvinyl phosphonate **P9** (dark blue), **P10** (light blue), and folic acid (orange). Cell viability (C) of MIO-M1 cells after 24 h with the polymers **P3** (green), **P4** (orange), **P9** (dark blue), and **P10** (light blue).

them in a manner orthogonal to the cholesterol moieties. Considering the previously mentioned reasons, the terminally initiated Huisgen cycloaddition is selected as the preferred method and executes under the same reaction conditions as those used for **P5** and **P6**. The synthesis of the azido-functionalized folic acid derivative **8** follows an established procedure described in the literature.[45] After complete purification of the polymer−biomolecule conjugate **P10**, confirmation of the successful coupling of the folic acid is achieved through meticulous ^{1}H NMR analysis. In the aromatic region of the NMR spectrum, distinct signals are observed at chemical shifts between 6.64 and 8.37 ppm, corresponding to characteristic resonances of folic acid. A signal attributed to the triazole moiety formed during the cycloaddition reaction is also identified at 7.56 ppm (Figure S28). However, owing to the relatively low proportion of folic acid within the polymer conjugate **P10** and the significantly reduced signal intensity of the functional groups in the NMR spectrum, a quantitative analysis of the functionalization degree is impossible. The covalent incorporation of the folic acid derivative **8** into the polymer is further confirmed by DOSY-NMR, as evidenced by its similar diffusion coefficient to that of the polyvinyl phosphonate (Figure S30). This observation not only indicates successful integration but also ensures the purity of the sample. Moreover, the polymer−biomolecule conjugate **P10** is analyzed using UV−vis and fluorescence spectroscopy. The UV−vis spectrum revealed two characteristic absorption bands in the range of 250−300 and 300−400 nm, corresponding to the $\pi-\pi^*$ and $n-\pi^*$ electronic transitions, respectively, of the pterin and *p*-amino benzoyl acid moieties of the folic acid (Figure 7A).[58] Moreover, the fluorescence spectra displayed an emission maximum at 465 nm, exhibiting a noticeable shift compared with the pure folic acid ($\lambda_{max} \approx 451$ nm) (Figure 7B). Notably, the exclusively cholesterol-functionalized polyvinyl phosphonate **P9** shows no signals in the fluorescence and UV−vis spectra. Furthermore, DLS determines that the polymer is capable of self-assembly and forms micelles with a cholesterol core (Figure S32).

Finally, the cytotoxicity of the unmodified polymers **P3** and **P4**, along with the cholesterol and folic acid-functionalized polyvinyl phosphonates **P9** and **P10**, is examined on cells. This assessment stands as a crucial determinant for the potential biomedical applications of these materials. Cell viability assays are performed using a spontaneously immortalized human Müller cell line (MIO-M1) by exposing the cells to different concentrations of the polymers (ranging from 5 to 1750 μg/mL) after 24 h. The resulting values of the assay are presented in Figure 7C. Up to a 500 μg/mL concentration, a cell viability of over 90% is observed for all polymers. Results show that TMS-protected terpolymer **P3** has a higher viability than 100%, but the cell viability decreases as the polymer concentration increases. Upon deprotection, the resulting polymer P(DAlVP-DEVP-DPrVP) **P4** demonstrates a significantly higher viability level of around 100% compared to **P3**, indicating the absence of toxicity. The cell viability of the cholesterol-functionalized polyvinyl phosphonate **P9** remains above 100% across the tested concentration range, indicating high biocompatibility. However, the addition of folic acid (**P10**) as an additional functionalized compound slightly decreases the obtained viability values. From a concentration of 1000 μg/mL onward, there is a noticeable decrease in the cell viability across all polymers. This decline is observed to be more dynamic in the case of polymers **P4** and **P10** compared to **P3** and **P9**. This can probably be attributed to the fact that higher molecular masses lead to an increase in cell membrane damage.[59] Nevertheless, it is evident that both deprotection from **P3** to **P4** and the functionalization of **P9** with folic acid to generate **P10** leads to a marked reduction in the cell viability in their respective cell tests (Figure S39). Preceding tests of polyvinyl phosphonates yielded promising results, with cell viability surpassing 50% in MTT assays.[21] However, the recent findings show that all four polymers exhibited a minimum of 78% cell viability following a 24 h treatment with a polymer concentration of 1 mg/mL. This finding provides valuable insights into subsequent cellular experiments. This further emphasizes the positive potential of these materials for biomedical applications. Additionally, a noteworthy observation emerges where data points surpassed 100%. These instances are construed as compelling evidence showcasing the favorable influence of the polymers on cell growth, imparting an intriguing dimension to their potential utility in the field of biomedicine. Overall, it can be concluded that all evaluated polyvinyl phosphonates (**P3**, **P4**, **P9**, and **P10**) display low toxicity. These findings suggest that these polymers are promising platforms for biological and medical applications.

3. CONCLUSIONS

In summary, the presented study reports the successful synthesis of α-allyl-ω-TMSpropargyl-*block-co*-polyvinyl phosphonate P(DAlVP-DEVP-DPrTMSVP) **P3**, employing the newly developed vinyl phosphonate DPrTMSVP via REM-

https://doi.org/10.1021/acs.macromol.3c02238
Macromolecules 2024, 57, 1438−1447

GTP. The sequential polymerization of the terpolymer is monitored via ^{1}H- and ^{31}P NMR spectroscopy, and the targeted structure is confirmed via DOSY-NMR spectroscopy as well as SEC-MALS. Additionally, the amphiphilic nature and self-assembly of the block copolymer are studied via DLS, revealing the formation of micelles of 100 nm size.

The modification of propargyl groups after quantitative cleavage of the TMS groups via the Huisgen click reaction with benzyl azide and 3-azido-7-hydroxy-coumarin is achieved and qualitatively demonstrated (Figure 8) via ^{1}H NMR spectroscopy. The attachment of the fluorescent dye to the polymer is further confirmed through UV−vis and fluorescence measurements of polymer **P6**. Moreover, a subsequent thiol-ene click reaction enabled almost quantitative conversion in functionalizing the allyl groups with the amino acid cysteine, opening the possibility of modifying the polymers with various peptide sequences. As a proof of concept for the functionalization approach using sequential, orthogonal click reactions on polyvinyl phosphonates toward potential biomedical applications, the terpolymer **P3** is modified through a thiol-ene click reaction with cholesterol, converting 75% of the allyl bonds in the polyvinyl phosphonate. Subsequent deprotection of the propargyl groups allows for the attachment of folic acid via AAC, which is confirmed through fluorescence and UV−vis measurements. Notably, the lipophilic character of cholesterol contributed to the formation of micelles in modified polymers **P9** and **P10**. Furthermore, unfunctionalized polymers **P3** and **P4** and biologically functionalized polymers **P9** and **P10** exhibit no cytotoxic behavior. Therefore, the investigated polyvinyl phosphonates exhibit essential fundamental characteristics. On the one hand, there is potential for further exploration through orthogonal modifications of *α*-allyl-*ω*-propargyl-*block-co*-polyvinyl phosphonate **P4**, allowing for the incorporation of diverse targeting groups, dyes, peptides, nucleobases, and other functionalities in various fields of application. On the other hand, research efforts can be dedicated to assess the suitability of the modified *α*-cholesteryl-*ω*-folate-*block-co*-polyvinyl phosphonate **P10**, for instance, as a linker for liposome-based drug delivery systems, comparing its performance with the well-established PEG variant.[60]

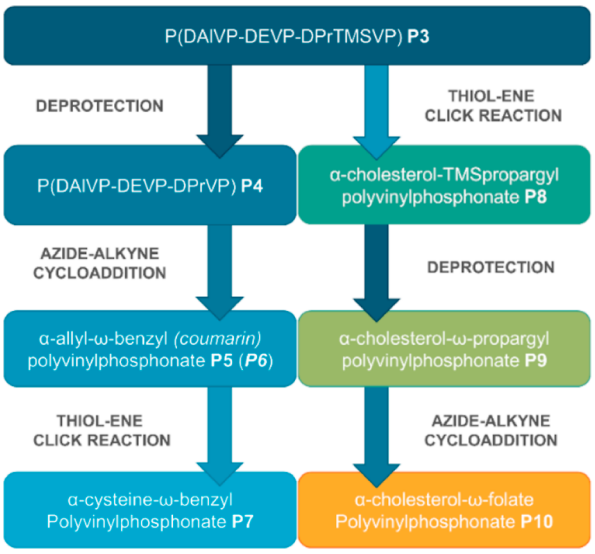

Figure 8. Schematic overview of synthesis cascades.

■ ASSOCIATED CONTENT

Supporting Information

The Supporting Information is available free of charge at https://pubs.acs.org/doi/10.1021/acs.macromol.3c02238.

Synthetic procedures of the synthesis, polymerization, and follow-up functionalization; and detailed characterization data (^{1}H-, ^{13}C-, ^{31}P-, and DOSY-NMR spectra, fluorescence spectra, UV−vis spectra, DLS measurements, elemental analysis, SEC-MALS traces, as well as cell viability assays) (PDF)

■ AUTHOR INFORMATION

Corresponding Author

Bernhard Rieger − *WACKER-Chair of Macromolecular Chemistry, Catalysis Research Center, Department of Chemistry, Technical University of Munich, 85748 Garching, Germany*; orcid.org/0000-0002-0023-884X; Email: rieger@tum.de

Authors

Kerstin Halama − *WACKER-Chair of Macromolecular Chemistry, Catalysis Research Center, Department of Chemistry, Technical University of Munich, 85748 Garching, Germany*

Molly Tzu-Yu Lin − *Institute for Ophthalmic Research, University of Tübingen, 72076 Tübingen, Germany*

Andreas Schaffer − *WACKER-Chair of Macromolecular Chemistry, Catalysis Research Center, Department of Chemistry, Technical University of Munich, 85748 Garching, Germany*

Marvin Foith − *WACKER-Chair of Macromolecular Chemistry, Catalysis Research Center, Department of Chemistry, Technical University of Munich, 85748 Garching, Germany*

Friederike Adams − *Institute for Ophthalmic Research, University of Tübingen, 72076 Tübingen, Germany; Chair of Macromolecular Materials and Fiber Chemistry, Institute of Polymer Chemistry, University of Stuttgart, 70569 Stuttgart, Germany*; orcid.org/0000-0002-4362-0387

Complete contact information is available at: https://pubs.acs.org/10.1021/acs.macromol.3c02238

Author Contributions

The manuscript was written through contributions of all authors. All authors have given approval for the final version of the manuscript.

Notes

The authors declare no competing financial interest.

■ ACKNOWLEDGMENTS

The authors are grateful to Fabian Späth, Anton Maier, and Marina Wittig for revising the manuscript. Furthermore, they thank Johanna Haimerl for her assistance in creating the graphical abstract and Brigita Bratić. F.A. and M.T.Y.L. are grateful for the funding received from the Federal Ministry of Education and Research (BMBF) and the Baden-Württemberg Ministry of Science, Research and Art, as part of the Excellence Strategy of the German Federal and State Governments.

■ REFERENCES

(1) Yen, S. K.; Jańczewski, D.; Lakshmi, J. L.; Dolmanan, S. B.; Tripathy, S.; Ho, V. H. B.; Vijayaragavan, V.; Hariharan, A.;

Padmanabhan, P.; Bhakoo, K. K.; et al. Design and Synthesis of Polymer-Functionalized NIR Fluorescent Dyes-Magnetic Nanoparticles for Bioimaging. *ACS Nano* **2013**, *7* (8), 6796−6805.
(2) Nicolas, J.; Mura, S.; Brambilla, D.; Mackiewicz, N.; Couvreur, P. Design, functionalization strategies and biomedical applications of targeted biodegradable/biocompatible polymer-based nanocarriers for drug delivery. *Chem. Soc. Rev.* **2013**, *42* (3), 1147−1235.
(3) Gai, M.; Simon, J.; Lieberwirth, I.; Mailänder, V.; Morsbach, S.; Landfester, K. A bio-orthogonal functionalization strategy for site-specific coupling of antibodies on vesicle surfaces after self-assembly. *Polym. Chem.* **2020**, *11* (2), 527−540.
(4) Cao, Y.; Dong, X.; Chen, X. Polymer-Modified Liposomes for Drug Delivery: From Fundamentals to Applications. *Pharmaceutics* **2022**, *14* (4), 778.
(5) Ghezzi, M.; Pescina, S.; Padula, C.; Santi, P.; Del Favero, E.; Cantù, L.; Nicoli, S. Polymeric micelles in drug delivery: An insight of the techniques for their characterization and assessment in biorelevant conditions. *J. Controlled Release* **2021**, *332*, 312−336.
(6) Hari, S. K.; Gauba, A.; Shrivastava, N.; Tripathi, R. M.; Jain, S. K.; Pandey, A. K. Polymeric micelles and cancer therapy: an ingenious multimodal tumor-targeted drug delivery system. *Drug Delivery Transl. Res.* **2023**, *13* (1), 135−163.
(7) Moulahoum, H.; Ghorbanizamani, F.; Zihnioglu, F.; Timur, S. Surface Biomodification of Liposomes and Polymersomes for Efficient Targeted Drug Delivery. *Bioconjugate Chem.* **2021**, *32* (8), 1491−1502.
(8) Veronese, F. M. Peptide and protein PEGylation: a review of problems and solutions. *Biomaterials* **2001**, *22* (5), 405−417.
(9) Mishra, P.; Nayak, B.; Dey, R. K. PEGylation in anti-cancer therapy: An overview. *Asian J. Pharm. Sci.* **2016**, *11* (3), 337−348.
(10) Dhiman, S.; Mishra, N.; Sharma, S. Development of PEGylated solid lipid nanoparticles of pentoxifylline for their beneficial pharmacological potential in pathological cardiac hypertrophy. *Artif. Cells, Nanomed., Biotechnol.* **2016**, *44* (8), 1901−1908.
(11) Gupta, V.; Bhavanasi, S.; Quadir, M.; Singh, K.; Ghosh, G.; Vasamreddy, K.; Ghosh, A.; Siahaan, T. J.; Banerjee, S.; Banerjee, S. K. Protein PEGylation for cancer therapy: bench to bedside. *J. Cell Commun. Signaling* **2019**, *13* (3), 319−330.
(12) Loiseau, F. A.; Hii, K. K.; Hill, A. M. Multigram Synthesis of Well-Defined Extended Bifunctional Polyethylene Glycol (PEG) Chains. *J. Org. Chem.* **2004**, *69* (3), 639−647.
(13) Hadjichristidis, N.; Iatrou, H.; Pitsikalis, M.; Pispas, S.; Avgeropoulos, A. Linear and non-linear triblock terpolymers. Synthesis, self-assembly in selective solvents and in bulk. *Prog. Polym. Sci.* **2005**, *30* (7), 725−782.
(14) Konishcheva, E.; Daubian, D.; Gaitzsch, J.; Meier, W. Synthesis of Linear ABC Triblock Copolymers and Their Self-Assembly in Solution. *Helv. Chim. Acta* **2018**, *101* (2), No. e1700287.
(15) Skandalis, A.; Sentoukas, T.; Giaouzi, D.; Kafetzi, M.; Pispas, S. Latest Advances on the Synthesis of Linear ABC-Type Triblock Terpolymers and Star-Shaped Polymers by RAFT Polymerization. *Polymers* **2021**, *13* (11), 1698.
(16) Kolb, H. C.; Finn, M. G.; Sharpless, K. B. Click Chemistry: Diverse Chemical Function from a Few Good Reactions. *Angew. Chem., Int. Ed.* **2001**, *40* (11), 2004−2021.
(17) Durmaz, H.; Sanyal, A.; Hizal, G.; Tunca, U. Double click reaction strategies for polymer conjugation and post-functionalization of polymers. *Polym. Chem.* **2012**, *3* (4), 825−835.
(18) Campos, L. M.; Killops, K. L.; Sakai, R.; Paulusse, J. M. J.; Damiron, D.; Drockenmuller, E.; Messmore, B. W.; Hawker, C. J. Development of Thermal and Photochemical Strategies for Thiol-Ene Click Polymer Functionalization. *Macromolecules* **2008**, *41* (19), 7063−7070.
(19) Javakhishvili, I.; Binder, W. H.; Tanner, S.; Hvilsted, S. Facile synthesis of linear-dendritic cholesteryl-poly(ε-caprolactone)-b-(l-lysine)G2 by thiol-ene and azide-alkyne "click" reactions. *Polym. Chem.* **2010**, *1* (4), 506−513.
(20) Schwarzenböck, C.; Nelson, P. J.; Huss, R.; Rieger, B. Synthesis of next generation dual-responsive cross-linked nanoparticles and their application to anti-cancer drug delivery. *Nanoscale* **2018**, *10* (34), 16062−16068.
(21) Schwarzenböck, C.; Schaffer, A.; Pahl, P.; Nelson, P. J.; Huss, R.; Rieger, B. Precise synthesis of thermoresponsive polyvinylphosphonate-biomolecule conjugates via thiol-ene click chemistry. *Polym. Chem.* **2018**, *9* (3), 284−290.
(22) Schwarzenböck, C.; Vagin, S. I.; Heinz, W. R.; Nelson, P. J.; Rieger, B. Studies on the Biocompatibility of Poly(diethyl vinylphosphonate) with a New Fluorescent Marker. *Macromol. Rapid Commun.* **2018**, *39* (15), 1800259.
(23) Altenbuchner, P. T.; Werz, P. D. L.; Schöppner, P.; Adams, F.; Kronast, A.; Schwarzenböck, C.; Pöthig, A.; Jandl, C.; Haslbeck, M.; Rieger, B. Next Generation Multiresponsive Nanocarriers for Targeted Drug Delivery to Cancer Cells. *Chem.—Eur. J.* **2016**, *22* (41), 14576−14584.
(24) Schaffer, A.; Weger, M.; Rieger, B. From lanthanide-mediated, high-precision group transfer polymerization of Michael-type monomers, to intelligent, functional materials. *Eur. Polym. J.* **2020**, *122*, 109385.
(25) Zhang, N.; Salzinger, S.; Rieger, B. Poly(vinylphosphonate)s with Widely Tunable LCST: A Promising Alternative to Conventional Thermoresponsive Polymers. *Macromolecules* **2012**, *45* (24), 9751−9758.
(26) Adams, F.; Pahl, P.; Rieger, B. Metal-Catalyzed Group-Transfer Polymerization: A Versatile Tool for Tailor-Made Functional (Co)Polymers. *Chem.—Eur. J.* **2018**, *24* (3), 509−518.
(27) Kränzlein, M.; Pehl, T. M.; Adams, F.; Rieger, B. Uniting Group-Transfer and Ring-Opening Polymerization-Block Copolymers from Functional Michael-Type Monomers and Lactones. *Macromolecules* **2021**, *54* (23), 10860−10869.
(28) Lanzinger, D.; Salzinger, S.; Soller, B. S.; Rieger, B. Poly(vinylphosphonate)s as Macromolecular Flame Retardants for Polycarbonate. *Ind. Eng. Chem. Res.* **2015**, *54* (6), 1703−1712.
(29) Adams, F.; Machat, M. R.; Altenbuchner, P. T.; Ehrmaier, J.; Pöthig, A.; Karsili, T. N. V.; Rieger, B. Toolbox of Nonmetallocene Lanthanides: Multifunctional Catalysts in Group-Transfer Polymerization. *Inorg. Chem.* **2017**, *56* (16), 9754−9764.
(30) Pahl, P.; Schwarzenböck, C.; Herz, F. A. D.; Soller, B. S.; Jandl, C.; Rieger, B. Core-First Synthesis of Three-Armed Star-Shaped Polymers by Rare Earth Metal-Mediated Group Transfer Polymerization. *Macromolecules* **2017**, *50* (17), 6569−6576.
(31) Kränzlein, M.; Pehl, T. M.; Halama, K.; Großmann, P. F.; Kratky, T.; Mühlbach, A. M.; Rieger, B. Azide-Modified Poly(diethyl vinylphosphonate) for Straightforward Graft-to Carbon Nanotube Functionalization. *Macromol. Mater. Eng.* **2023**, *308* (6), 2200635.
(32) Adams, F.; Pschenitza, M.; Rieger, B. Yttrium-Catalyzed Synthesis of Bipyridine-Functionalized AB-Block Copolymers: Micellar Support for Photocatalytic Active Rhenium-Complexes. *ChemCatChem* **2018**, *10* (19), 4309−4316.
(33) Schaffer, A.; Kränzlein, M.; Rieger, B. Synthesis and Application of Functional Group-Bearing Pyridyl-Based Initiators in Rare Earth Metal-Mediated Group Transfer Polymerization. *Macromolecules* **2020**, *53* (11), 4345−4354.
(34) Pehl, T. M.; Kränzlein, M.; Adams, F.; Schaffer, A.; Rieger, B. C-H Bond Activation of Silyl-Substituted Pyridines with Bis(Phenolate)Yttrium Catalysts as a Facile Tool towards Hydroxyl-Terminated Michael-Type Polymers. *Catalysts* **2020**, *10* (4), 448.
(35) Halama, K.; Schaffer, A.; Rieger, B. Allyl group-containing polyvinylphosphonates as a flexible platform for the selective introduction of functional groups via polymer-analogous transformations. *RSC Adv.* **2021**, *11* (61), 38555−38564.
(36) Pehl, T. M.; Adams, F.; Kränzlein, M.; Rieger, B. Expanding the Scope of Organic Radical Polymers to Polyvinylphosphonates Synthesized via Rare-Earth Metal-Mediated Group-Transfer Polymerization. *Macromolecules* **2021**, *54* (9), 4089−4100.
(37) Saurwein, A.; Schaffer, A.; Wieser, C.; Rieger, B. Synthesis, characterisation and functionalisation of BAB-type dual-responsive nanocarriers for targeted drug delivery: evolution of nanoparticles

https://doi.org/10.1021/acs.macromol.3c02238
Macromolecules 2024, 57, 1438−1447

based on 2-vinylpyridine and diethyl vinylphosphonate. *RSC Adv.* **2021**, *11* (3), 1586−1594.
(38) Schaffer, A.; Kränzlein, M.; Rieger, B. Precise Synthesis of Poly(dimethylsiloxane) Copolymers through C-H Bond-Activated Macroinitiators via Yttrium-Mediated Group Transfer Polymerization and Ring-Opening Polymerization. *Macromolecules* **2020**, *53* (19), 8382−8392.
(39) Adams, F.; Altenbuchner, P. T.; Werz, P. D. L.; Rieger, B. Multiresponsive micellar block copolymers from 2-vinylpyridine and dialkylvinylphosphonates with a tunable lower critical solution temperature. *RSC Adv.* **2016**, *6* (82), 78750−78754.
(40) Schwarzenböck, C.; Schaffer, A.; Nößner, E.; Nelson, P. J.; Huss, R.; Rieger, B. Fluorescent Polyvinylphosphonate Bioconjugates for Selective Cellular Delivery. *Chem.—Eur. J.* **2018**, *24* (11), 2584−2587.
(41) Yang, H.; Sun, A.; Chai, C.; Huang, W.; Xue, X.; Chen, J.; Jiang, B. Synthesis and post-functionalization of a degradable aliphatic polyester containing allyl pendent groups. *Polymer* **2017**, *121*, 256−261.
(42) Ruwizhi, N.; Aderibigbe, B. A. The Efficacy of Cholesterol-Based Carriers in Drug Delivery. *Molecules* **2020**, *25* (18), 4330.
(43) Misiak, P.; Markiewicz, K. H.; Szymczuk, D.; Wilczewska, A. Z. Polymeric Drug Delivery Systems Bearing Cholesterol Moieties: A Review. *Polymers* **2020**, *12* (11), 2620.
(44) Wang, W.-Y.; Cao, Y.-X.; Zhou, X.; Wei, B. Delivery of folic acid-modified liposomal curcumin for targeted cervical carcinoma therapy. *Drug Des., Dev. Ther.* **2019**, *13*, 2205−2213.
(45) Liu, L.; Zheng, M.; Renette, T.; Kissel, T. Modular Synthesis of Folate Conjugated Ternary Copolymers: Polyethylenimine-graft-Polycaprolactone-block-Poly(ethylene glycol)-Folate for Targeted Gene Delivery. *Bioconjugate Chem.* **2012**, *23* (6), 1211−1220.
(46) Kumar, P.; Huo, P.; Liu, B. Formulation Strategies for Folate-Targeted Liposomes and Their Biomedical Applications. *Pharmaceutics* **2019**, *11* (8), 381.
(47) Soller, B. S.; Salzinger, S.; Jandl, C.; Pöthig, A.; Rieger, B. C-H Bond Activation by σ-Bond Metathesis as a Versatile Route toward Highly Efficient Initiators for the Catalytic Precision Polymerization of Polar Monomers. *Organometallics* **2015**, *34* (11), 2703−2706.
(48) Kaneko, H.; Nagae, H.; Tsurugi, H.; Mashima, K. End-Functionalized Polymerization of 2-Vinylpyridine through Initial C-H Bond Activation of N-Heteroaromatics and Internal Alkynes by Yttrium Ene-Diamido Complexes. *J. Am. Chem. Soc.* **2011**, *133* (49), 19626−19629.
(49) Huisgen, R. 1.3-Dipolare Cycloadditionen Rückschau und Ausblick. *Angew. Chem.* **1963**, *75* (13), 604−637.
(50) Tsurkan, M. V.; Chwalek, K.; Prokoph, S.; Zieris, A.; Levental, K. R.; Freudenberg, U.; Werner, C. Defined Polymer-Peptide Conjugates to Form Cell-Instructive starPEG-Heparin Matrices In Situ. *Adv. Mater.* **2013**, *25* (18), 2606−2610.
(51) Colak, B.; Wu, L.; Cozens, E. J.; Gautrot, J. E. Modulation of Thiol-Ene Coupling by the Molecular Environment of Polymer Backbones for Hydrogel Formation and Cell Encapsulation. *ACS Appl. Bio Mater* **2020**, *3* (9), 6497−6509.
(52) Sharma, S.; Pukale, S. S.; Sahel, D. K.; Agarwal, D. S.; Dalela, M.; Mohanty, S.; Sakhuja, R.; Mittal, A.; Chitkara, D. Folate-Targeted Cholesterol-Grafted Lipo-Polymeric Nanoparticles for Chemotherapeutic Agent Delivery. *AAPS PharmSciTech* **2020**, *21* (7), 280.
(53) Wang, H.; Zhao, P.; Liang, X.; Gong, X.; Song, T.; Niu, R.; Chang, J. Folate-PEG coated cationic modified chitosan - Cholesterol liposomes for tumor-targeted drug delivery. *Biomaterials* **2010**, *31* (14), 4129−4138.
(54) Joshi, R.; Adhikari, S.; Patro, B. S.; Chattopadhyay, S.; Mukherjee, T. Free radical scavenging behavior of folic acid: evidence for possible antioxidant activity. *Free Radical Biol. Med.* **2001**, *30* (12), 1390−1399.
(55) Fairbanks, B. D.; Sims, E. A.; Anseth, K. S.; Bowman, C. N. Reaction Rates and Mechanisms for Radical, Photoinitated Addition of Thiols to Alkynes, and Implications for Thiol-Yne Photopolymerizations and Click Reactions. *Macromolecules* **2010**, *43* (9), 4113−4119.
(56) Lowe, A. B.; Hoyle, C. E.; Bowman, C. N. Thiol-yne click chemistry: A powerful and versatile methodology for materials synthesis. *J. Mater. Chem.* **2010**, *20* (23), 4745−4750.
(57) Stolz, R. M.; Northrop, B. H. Experimental and Theoretical Studies of Selective Thiol-Ene and Thiol-Yne Click Reactions Involving N-Substituted Maleimides. *J. Org. Chem.* **2013**, *78* (16), 8105−8116.
(58) Baibarac, M.; Smaranda, I.; Nila, A.; Serbschi, C. Optical properties of folic acid in phosphate buffer solutions: the influence of pH and UV irradiation on the UV-VIS absorption spectra and photoluminescence. *Sci. Rep.* **2019**, *9* (1), 14278.
(59) Correia, J. S.; Mirón-Barroso, S.; Hutchings, C.; Ottaviani, S.; Somuncuoğlu, B.; Castellano, L.; Porter, A. E.; Krell, J.; Georgiou, T. K. How does the polymer architecture and position of cationic charges affect cell viability? *Polym. Chem.* **2023**, *14* (3), 303−317.
(60) Zhao, X. B.; Muthusamy, N.; Byrd, J. C.; Lee, R. J. Cholesterol as a bilayer anchor for PEGylation and targeting ligand in folate receptor targeted liposomes. *J. Pharm. Sci.* **2007**, *96* (9), 2424−2435.

https://doi.org/10.1021/acs.macromol.3c02238
Macromolecules 2024, 57, 1438−1447